

See discussions, stats, and author profiles for this publication at: <https://www.researchgate.net/publication/23237376>

A Guided-Ion Beam Study of the $O + (4S) + NH_3$ System at Hyperthermal Energies †

ARTICLE in THE JOURNAL OF PHYSICAL CHEMISTRY A · OCTOBER 2008

Impact Factor: 2.69 · DOI: 10.1021/jp803120z · Source: PubMed

CITATIONS

6

READS

25

3 AUTHORS:



Dale Levandier

Physical Sciences Inc.

51 PUBLICATIONS 757 CITATIONS

SEE PROFILE



Yu-Hui Chiu

69 PUBLICATIONS 903 CITATIONS

SEE PROFILE



Rainer Dressler

Spectral Sciences Incorporated

113 PUBLICATIONS 1,430 CITATIONS

SEE PROFILE

REPORT DOCUMENTATION PAGE				Form Approved OMB No. 0704-01-0188	
<p>The public reporting burden for this collection of information is estimated to average 1 hour per response, including the time for reviewing instructions, searching existing data sources, gathering and maintaining the data needed, and completing and reviewing the collection of information. Send comments regarding this burden estimate or any other aspect of this collection of information, including suggestions for reducing the burden to Department of Defense, Washington Headquarters Services Directorate for Information Operations and Reports (0704-0188), 1215 Jefferson Davis Highway, Suite 1204, Arlington VA 22202-4302. Respondents should be aware that notwithstanding any other provision of law, no person shall be subject to any penalty for failing to comply with a collection of information if it does not display a currently valid OMB control number.</p> <p>PLEASE DO NOT RETURN YOUR FORM TO THE ABOVE ADDRESS.</p>					
1. REPORT DATE (DD-MM-YYYY) 14-07-2008		2. REPORT TYPE REPRINT		3. DATES COVERED (From - To)	
4. TITLE AND SUBTITLE A Guided-Ion Beam Study of the $O^+(^4S) + NH_3$ System at Hyperthermal Energies				5a. CONTRACT NUMBER	
				5b. GRANT NUMBER	
				5c. PROGRAM ELEMENT NUMBER 61102F	
6. AUTHORS Dale J. Levandier* Yu-Hui-Chiu Rainer A. Dressler				5d. PROJECT NUMBER 2303	
				5e. TASK NUMBER RS	
				5f. WORK UNIT NUMBER A1	
7. PERFORMING ORGANIZATION NAME(S) AND ADDRESS(ES) Air Force Research Laboratory /RVBXT 29 Randolph Road Hanscom AFB, MA 01731-3010				8. PERFORMING ORGANIZATION REPORT NUMBER AFRL-RV-HA-TR-2008-1119	
9. SPONSORING/MONITORING AGENCY NAME(S) AND ADDRESS(ES)				10. SPONSOR/MONITOR'S ACRONYM(S) AFRL/RVBXT	
				11. SPONSOR/MONITOR'S REPORT NUMBER(S)	
12. DISTRIBUTION/AVAILABILITY STATEMENT Approved for Public Release; distribution unlimited.					
13. SUPPLEMENTARY NOTES Reprinted from: J. Phys Chem. A (2008) 112, 9601-9606 (Part of the Stephen R. Leone Festschrift) © 2008 American Chemical Society *Boston College Institute for Scientific Research, 140 Commonwealth Ave., Chestnut Hill, MA, 02167					
14. ABSTRACT We have measured absolute cross sections for the reaction of ground-state O^+ with ammonia at collision energies in the range from near-thermal to approximately 15 eV, using the guided-ion beam (GIB) method. Measurements were also performed using ammonia- d_3 to aid in mass assignments. The reaction is dominated at low collision energies by charge transfer; however, the cross section for this exothermic channel is rather small, decreasing sharply with energy from $\sim 40 \text{ \AA}^2$ for normal ammonia at near-thermal energies and leveling off at 3.7 \AA^2 above 6 eV; the cross section is slightly smaller for ammonia- d_3 . Other channels, corresponding to the production of NH_2^+ and NO^+ and possibly OH^+ , were detected. The NO^+ channel, although nominally exothermic, is very small and exhibits a threshold of ~ 7 eV. Product recoil velocity distributions were also determined at selected collision energies, using GIB time-of-flight methods.					
15. SUBJECT TERMS Guided-ion beam Oxygen-ammonia collisions Hyperthermal reactions Charge transfer Reaction cross section					
16. SECURITY CLASSIFICATION OF:			17. LIMITATION OF ABSTRACT	18. NUMBER OF PAGES	19a. NAME OF RESPONSIBLE PERSON
a. REPORT	b. ABSTRACT	c. THIS PAGE			Yu-Hui Chiu
UNCL	UNCL	UNCL	UNCL		19b. TELEPHONE NUMBER (Include area code)

20081222157

A Guided-Ion Beam Study of the $\text{O}^+(\text{}^4\text{S}) + \text{NH}_3$ System at Hyperthermal Energies[†]Dale J. Levandier,^{*,‡,§} Yu-Hui Chiu,[‡] and Rainer A. Dressler^{‡,‡}

Air Force Research Laboratory, Space Vehicles Directorate, Hanscom AFB, Massachusetts 01731, and Boston College Institute for Scientific Research, 140 Commonwealth Avenue, Chestnut Hill, Massachusetts 02159

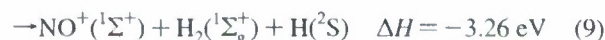
Received: April 10, 2008; Revised Manuscript Received: July 14, 2008

We have measured absolute cross section for the reaction of ground-state O^+ with ammonia at collision energies in the range from near-thermal to approximately 15 eV, using the guided-ion beam (GIB) method. Measurements were also performed using ammonia- d_3 to aid in mass assignments. The reaction is dominated at low collision energies by charge transfer; however, the cross section for this exothermic channel is rather small, decreasing sharply with energy from $\sim 40 \text{ \AA}^2$ for normal ammonia at near-thermal energies and leveling off at 3.7 \AA^2 above 6 eV; the cross section is slightly smaller for ammonia- d_3 . Other channels, corresponding to the production of NH_2^+ and NO^+ , and possibly OH^+ , were detected. The NO^+ channel, although nominally exothermic, is very small and exhibits a threshold at $\sim 7 \text{ eV}$. Product recoil velocity distributions were also determined at selected collision energies, using GIB time-of-flight methods.

Introduction

Hyperthermal reactions of atomic cations with ammonia are interesting both from a fundamental standpoint, in the ongoing efforts to understand the detailed mechanisms of chemical reactions, and in a broader physical sense, for example, in the quest to understand the interactions of one of the important molecules in interstellar media.¹ Modern computational methods such as direct dynamics calculations² are becoming powerful tools for studying chemistry, and benefit from having experimental benchmarks for comparison. In recent direct dynamics simulations by Sun and Schatz,³ excellent quantitative agreement was obtained with experiments on hyperthermal reactions of $\text{O}^+(\text{}^4\text{S}) + \text{CH}_4$ done in our group.⁴ Interestingly, these calculations showed, and the experiments confirmed, that many of the energetically accessible product channels were observed, including many that had not previously been seen. The aim of the present study is to provide a further basis of comparison for theoretical work.

Previous experimental investigation of the $\text{O}^+ + \text{NH}_3$ system is limited to an early selected-ion flow tube (SIFT) survey in which only charge transfer was observed, occurring at a rate of $1.2 \times 10^{-9} \text{ cm}^3/\text{s}$.⁵ High level *ab initio* calculations on the lowest doublet and quartet potential energy surfaces (PESs) have been performed for $\text{O}^+ + \text{NH}_3$.⁶ This work suggests that additional channels, leading to the formation of NH_2^+ (not distinguishable in the experiment) and H_2O^+ are accessible on the quartet PES, and that NH^+ , H_2NO^+ , and HNO^+ derive on the doublet PES.⁶ These products, along with their ground-state energetics, are listed below with several other exothermic channels:⁷



In this paper we present the results of a guided-ion beam (GIB) study of the $\text{O}^+ + \text{NH}_3$ reaction system, in which we have measured absolute cross sections for the observed reaction channels at near-thermal to hyperthermal collision energies. We have also determined recoil velocity distributions for product ions at selected collision energies. Experiments were carried out using normal and perdeuteroammonia because of the prospect of coincident ion masses.

Experimental Section

The GIB instrument used in the present study has been explained in detail previously,⁸ so only a brief description follows. The system is a tandem mass spectrometer that features a two-stage radio-frequency (rf) octopole ion guide located between the mass filters. The ion guide–collision cell assembly has been updated and is a duplicate of one described elsewhere.⁹ The first and second stages of the new ion guide are of lengths 8.6 and 19.6 cm, respectively, and the collision cell has a nominal length of 5 cm.

The $\text{O}^+(\text{}^4\text{S})$ beam is formed by dissociative ionization due to electron impact at $\sim 20 \text{ eV}$ on carbon dioxide. The primary ions are mass-selected in a Wien filter, and are injected into the first octopole at the desired kinetic energy. While in the first octopole, the ions pass through the collision cell, which is filled with the NH_3 target gas. At the exit of the collision cell, unreacted primary ions and ions produced by reactions with ammonia pass into the second octopole stage. The ions pass

[†] Part of the "Stephen R. Leone Festschrift".

* Corresponding author.

[‡] Hanscom AFB.[§] Boston College Institute for Scientific Research.[‡] Current address: Spectral Sciences, Inc., 4 Fourth Ave., Burlington, MA 01803-3304.

from the second octopole into a quadrupole mass filter for analysis. A ring-shaped electrode that surrounds the first octopole at the entrance of the collision cell is kept ~ 100 V above the direct current (dc) potential of the octopole, so that the small penetrating field (~ 0.1 V) reflects thermal product ions with laboratory velocities in the backward direction, thus allowing all but a negligible number of thermal product ions to be collected and included in the determination of the absolute cross sections. Ions with higher backward laboratory velocities are similarly reflected at the octopole injection lens, except at the very lowest beam energies. The ion beam energy is known to better than ± 0.1 eV, with 0.25–0.3 eV full width at half-maximum (fwhm) energy spread, as measured by retarding potential and time-of-flight (TOF) methods.

Secondary reactions in the collision cell occur in large part because of the very efficient rates of reaction for the thermal product ions with ammonia.¹⁰ These reactions are minimized by maintaining low collision cell pressures, in the range of 0.11–0.16 mTorr, by accelerating thermal ions out of the first octopole with a small (~ 0.4 V) negative bias on the second octopole relative to the first, and by periodically turning off the rf potential to allow trapped low-energy ions to escape the octopole volume.¹¹

As in previous work,^{4,8} absolute cross sections are obtained by integrating the signal intensities for product and transmitted primary ions, observing the target gas pressure, and applying the Lambert–Beer expression. A correction is applied that accounts for reactions of the ion beam with the residual vacuum chamber pressure of the target gas that resides within the octopole; the correction is obtained by measuring product ion signals resulting when the target gas is diverted directly into the chamber, and typically amounts to 10–15% of the uncorrected signal. The instrument was calibrated using the $\text{Ar}^+ + \text{D}_2 \rightarrow \text{ArD}^+ + \text{D}$ reaction;^{8,12} errors in the absolute cross sections are estimated to be $\pm 30\%$.

Product ion TOF spectra are obtained by using a pulsed O^+ beam, with a 5–6 μs fwhm beam pulse width, and measuring the arrival time of product ions at the detector. The pulsing frequency, here 3000 Hz, is adjusted to ensure that the bulk of product ions have sufficient time to exit the octopole, including those ions reflected by the ring electrode described above. The residual of very slow ions, which would accumulate and cause a background signal in subsequent pulse cycles, is eliminated from the octopole at the end of each cycle by briefly turning off the octopole rf voltage.

Results

Figures 1 and 2 show the absolute cross sections for the ionic products derived from reactions of O^+ with NH_3 and ND_3 , respectively, at kinetic energies (E_T) in the range from near-thermal to ~ 15 eV. In Figure 1, the cross sections for $\text{O}^+ + \text{NH}_3$ derived from the SIFT thermal rate constant, attributed solely to charge transfer,⁵ and the average dipole orientation (ADO) model^{13,14} are shown.

The data in Figures 1 and 2 indicate that no fewer than four reaction channels occur in the $\text{O}^+ + \text{NH}_3$ system, the assignments of which are discussed in more detail below. As mentioned above, the difficulty in attributing the product ion masses to specific reaction channels resides in the mass coincidences among several prospective products, as well as the primary ion and secondary products. Reactions with ammonia- d_3 and TOF studies were used to address some of these issues.

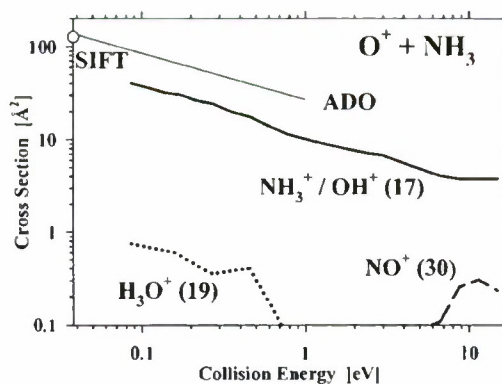


Figure 1. Absolute cross sections for reactions of O^+ with NH_3 as a function of collision, or relative, energy (E_T). The cross sections for individual product channels are labeled with the ion species assigned to the detected product masses (in parentheses, in amu). The thin solid line is the ADO cross section (refs 13 and 14), and the circle corresponds to the rate constant for $\text{O}^+ + \text{NH}_3$ reaction measured in SIFT experiments (ref 5).

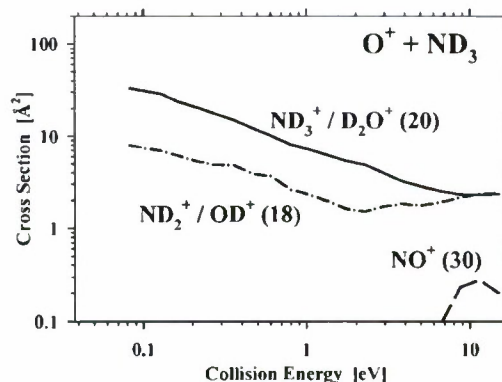


Figure 2. Absolute cross sections for reactions of O^+ with ND_3 as a function of collision, or relative, energy (E_T). The cross sections for individual product channels are labeled with the ion species assigned to the detected product masses (in parentheses, in amu). The data are plotted on the same scale as those in Figure 1, for ease of comparison.

Two of the observed reaction channels may be assigned unequivocally. In both Figures 1 and 2, a cross section is observed that corresponds to the production of a 30 amu product, NO^+ . This channel is very small, with a cross section that does not exceed 0.3 Å^2 at any point, and giving rise to no appreciable product below ~ 7 eV. At the highest energies observed, this cross section appears to diminish. The other obvious reaction product is H_3O^+ , observed clearly only in NH_3 reactions since it is also a small channel and there are no coincident ions (for ND_3 reactions, D_3O^+ coincides with ND_4^+ , a secondary product). The H_3O^+ cross section is observed only at low collision energy, where it drops sharply from $\sim 0.8 \text{ Å}^2$ to negligible levels with increasing energy.

The largest cross sections in Figures 1 and 2 involve ion products of 17 and 20 amu, respectively. The early SIFT work on normal ammonia⁵ would suggest that these correspond to charge transfer, and the energy dependence of these cross sections, with a sharp decline with energy at low collision energies and a leveling off at higher E_T , is typical of exothermic charge transfer in polyatomic systems. In either case, however, there are coincident ions, namely OH^+ and D_2O^+ , respectively, which are discussed below. At low energy, the $\text{NH}_3^+/\text{OH}^+$ cross section is $\sim 40 \text{ Å}^2$, substantially less than the SIFT and ADO results, and decreases until it levels off at a value of 3.7 Å^2 above 6 eV. The $\text{ND}_3^+/\text{D}_2\text{O}^+$ cross section is $\sim 33 \text{ Å}^2$ at low

energy, and levels off at 2.4 \AA^2 at higher energy. The remaining cross section, observed in ND_3 reactions, involves product ions of mass 18 amu, possibly ND_2^+ and/or OD^+ . This cross section is smaller than but of very similar form to the ND_3^+/D_2O^+ cross section, beginning at $\sim 8 \text{ \AA}^2$ at low energy, and falling to a value of 2.4 \AA^2 at higher energy, with a slightly lower region at 2–3 eV. Obviously, this channel cannot be distinguished in NH_3 reactions since the prospective products correspond in mass either to the ion beam (NH_3^+) or the main product (OH^+).

The small but non-negligible signal due to secondary reactions of product ions with $NH_3(ND_3)$ to give, largely, $NH_4^+(ND_4^+)$ was treated as follows. For the ND_3 case, the secondary “cross section” was added to the 20 and 18 amu cross sections in the proportion of these cross sections. This proportional partitioning is done since the rate constants for the relevant secondary reactions have sufficient scatter among published¹⁰ values as to justify an approximation of their being equal, for present purposes. The same branching fraction was assumed for the NH_3 case, and was used to derive a contribution to the charge transfer cross section from the measured secondary signal. A pressure dependence study was performed at selected kinetic energies, in which the NH_3^+ cross section was measured at a series of target gas pressures, and the results extrapolated to zero pressure; these results were found to agree with the above procedure to well within the cited error limits.

Figures 3 and 4 show TOF results at selected collision energies for the 17 amu product of $O^+ + NH_3$ reactions and the 20 amu product of $O^+ + ND_3$ reactions, respectively. The plots are product ion laboratory velocity distributions for the velocity component parallel to the ion beam, $f(v_p)$, and are obtained by transforming the raw product flight time data. The thin vertical dotted line in each spectrum indicates the velocity of the center of mass of the colliding species, V_{CM} . This velocity comprises the origin of the center-of-mass (CM) reference frame, with faster ions corresponding to forward-scattered products (the ion beam direction being defined as “forward”), and slower ions being back-scattered. The scattering intensities in the transformed spectra are normalized to a maximum of 100.

The velocity distributions in Figure 3, at collision energies of 1.55, 2.58, and 5.15 eV, show that ions of mass 17 amu deriving from reactions with normal ammonia, i.e., NH_3^+/OH^+ , are scattered in both the forward and backward directions. The dominant peak at low laboratory velocity in each spectrum corresponds to ions with essentially a thermal velocity distribution. The small forward scattered component diminishes at higher collision energy. The 2.58 eV plot includes a second velocity distribution (dashed curve) obtained for the same product(s) with a low octopole trapping potential, U_{RF} ($\sim 10 V_{rms}$, as compared to $100 V_{rms}$ normally). This TOF spectrum, which is scaled (by eye) so that its high velocity edge overlaps the same region in the normal spectrum, exhibits a pronounced drop in relative intensity in the region near V_{CM} , indicating that the missing signal, due to ions not retained by the lower trapping field, is the result of wide-angle scattering as opposed to products associated with low recoil velocities in the CM frame.

The velocity distributions in Figure 4 were obtained in experiments at the same laboratory ion beam energies as in Figure 3. The TOF spectra of the mass 20 amu ammonia- d_3 products, ND_3^+/D_2O^+ , are similar to those in Figure 3, the most remarkable difference being the slight peak in the forward scattered components in Figure 3, particularly evident at velocities just greater than 6000 and 9000 m/s in the data at $E_T = 2.58$ and 5.15 eV, respectively. Given that the H_2O^+/D_2O^+ channel is negligible (see below), and that the data in Figures

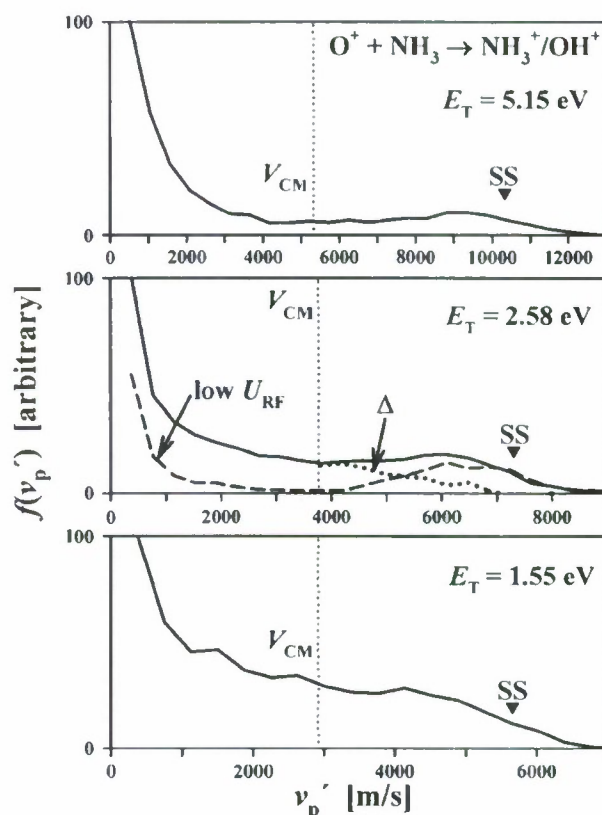


Figure 3. Laboratory velocity distributions for the NH_3^+/OH^+ (17 amu) product of $O^+ + NH_3$ reactions, transformed from ion TOF measurements at the collision energies shown. In each plot, the heavy solid curves comprise data obtained with normal RF trapping potential (U_{RF}), the thin vertical dotted line indicates the velocity of the CM of the collision system (V_{CM}), and the downward pointing triangles indicate the spectator stripping (SS) limit for OH^+ formation. In the middle frame, for $E_T = 2.58$ eV, the heavy dashed curve represents data obtained with low U_{RF} . This curve is scaled (by eye) so that the high velocity edges of the data for normal and low U_{RF} overlap. The heavy dotted curve represents the difference (Δ) between the normal and low U_{RF} data for the forward direction.

3 and 4 are otherwise similar, it is reasonable to consider whether this forward-scattered component corresponds to OH^+ . Efficient formation of OH^+ at higher collision energies would be most likely to occur in a stripping mechanism, resulting in forward-scattered product ions. The triangles in each frame of Figure 3 indicate the nominal spectator stripping (SS) velocity;¹⁵ the SS model represents a limit of the stripping mechanism characterized by an association reaction between the incident ion and the transferred atom.

If the forward scattered peak observed in Figure 3 is in part due to OH^+ formation, the low- U_{RF} data at $E_T = 2.58$ eV may be used to determine an upper limit of the contribution of OH^+ formation to the 17 amu cross section for the $O^+ + NH_3$ system at this collision energy. The forward-scattered low- U_{RF} component represents 20% of the integrated velocity spectrum obtained at normal U_{RF} . The heavy dotted curve in the respective frame, labeled “ Δ ”, is the difference between the two, and exhibits similar tailing to high velocity as seen in the $O^+ + ND_3$ TOF data in Figure 4. Also noteworthy in Figures 3 and 4 is that no significant forward “superelastic” scattering is observed; the same may be expected in the backward direction for complex-mediated reactions; therefore the absolute cross sections reported above should not be substantially affected at low energy by losses in the ion guide due to products with high backward kinetic energy release.

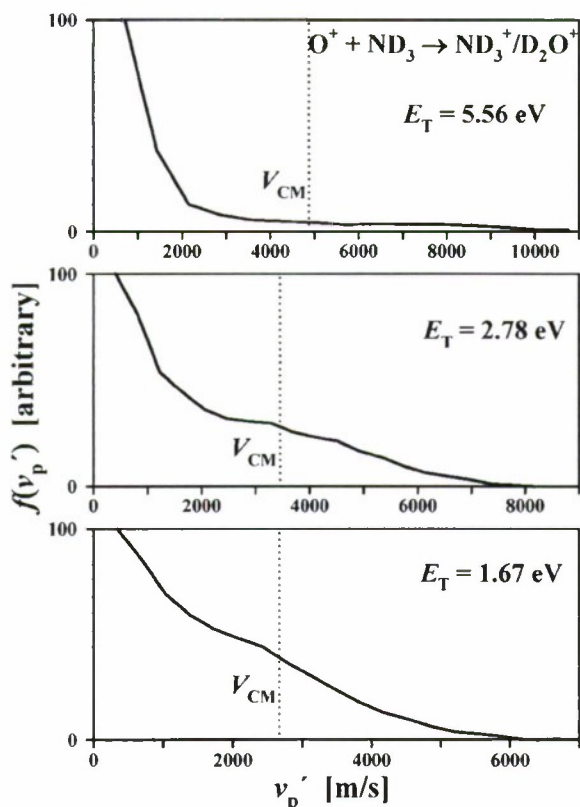


Figure 4. Laboratory velocity distributions for the $\text{ND}_3^+/\text{D}_2\text{O}^+$ (20 amu) product of $\text{O}^+ + \text{ND}_3$ reactions, transformed from ion TOF measurements at the collision energies shown. In each plot, the dotted line indicates the velocity of the CM of the collision system (V_{CM}).

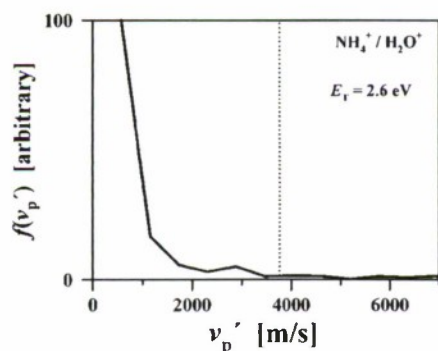


Figure 5. The laboratory velocity distribution for the 18 amu ions observed in the study of $\text{O}^+ + \text{NH}_3$ reactions at $E_T = 2.6$ eV. The dotted line indicates the velocity of the center of mass of the collision system (V_{CM}). The prominent peak at low velocity suggests that the 18 amu signal is due overwhelmingly to secondary reactions that produce NH_4^+ .

Figure 5 is a velocity spectrum of 18 amu ions derived from $\text{O}^+ + \text{NH}_3$ collisions at 2.58 eV collision energy. These TOF data are dominated by ions with a thermal velocity spectrum (the small bump at ~ 3000 m/s is representative of scatter in the data), and point very clearly to the NH_4^+ ion, which is expected to be a prominent product of secondary reactions in this system.¹⁰ Reactions in which H_2O^+ ions are predominantly scattered in the backward direction would be expected to occur infrequently, given that such rebounding collisions occur only in head-on collisions. Also, low-impact parameter collisions would be expected to be associated with high degrees of energy transfer, leading to forward scattering. Clearly, the TOF data in Figure 5 indicate that the probability for H_2O^+ forward scattering is very small. The above-mentioned pressure depen-

dence study also suggested that the 18 amu ions observed in the $\text{O}^+ + \text{NH}_3$ reactions are the result of secondary reactions, and are not due to H_2O^+ .

If the normal and perdeuteroammonia exhibit similar tendencies, it follows from the examination of Figure 5 that the cross section for the 20 amu channel in Figure 2 is due to charge transfer, yielding ND_3^+ . The similarity of form between this cross section and the 17 amu curve in Figure 1 suggests that the latter is also predominantly due to charge transfer. This is supported by the above analysis of the $E_T = 2.58$ eV TOF data in Figure 3, which suggests that OH^+ is at best a minor contributor to the 17 amu signal.

The upper limit established for the OH^+ contribution to the 17 amu signal from $\text{O}^+ + \text{NH}_3$ reactions at $E_T = 2.58$ eV is small but non-negligible. This is relevant to the assignment of the 18 amu product ions from $\text{O}^+ + \text{ND}_3$ reactions, shown in Figure 2. Efforts to gain insight into the relative contributions of ND_2^+ and OD^+ using TOF measurements (at $E_T = 1$ eV; not shown here), in which backscattered products were the more prevalent, were not conclusive. The suggestion of a stripping mechanism for OH^+ formation and the observation of a larger backscattered component in 18 amu products of $\text{O}^+ + \text{ND}_3$ reactions points to a greater contribution of ND_2^+ at lower energies, while the upper limit for OH^+ , indicated above, allows for a substantial contribution of OD^+ to the 18 amu cross section at $E_T = 2.6$ eV.

Discussion

The present study of hyperthermal reactions of O^+ with ammonia indicate that several product channels occur, namely those producing the ions NH_3^+ , NH_2^+ , OH^+ , H_3O^+ , and NO^+ (eqs 1, 2, 3, 6, and 9, respectively). The H_2O^+ product (eq 5) was below the sensitivity of the present experiment (0.1 \AA^2).

Below 9 eV, charge transfer is the largest cross section observed in this study. The cross section is substantially less than the ADO capture cross section,^{13,14} and diminishes to a small value at higher collision energies. As an exothermic charge transfer process, the reaction might be expected to occur in large impact parameter collisions in which typically no momentum transfer occurs. The small cross section, particularly at large collision energies where the capture mechanism is not relevant, suggests that this long-range mechanism is not efficient, which may be restated as there being only small coupling between the entrance and exit charge transfer channels. This small coupling may be explained by the requirement that the long-range charge transfer mechanism is quasi-resonant, and that the magnitude of the coupling depends on the near-resonant entrance and exit vibronic states having non-negligible Franck–Condon overlap.¹⁶ The photoelectron spectrum of ammonia¹⁷ shows that there is no Franck–Condon overlap for ionization to a state at the energy corresponding to the oxygen atom ionization potential, 13.62 eV.⁷

The decline in the charge transfer cross section from its highest point at low collision energy has an energy dependence similar to that for the ADO model, which points to a complex-mediated charge transfer reaction, or a capture mechanism, at low collision energy. The TOF data in Figures 3 and 4 are consistent with this scenario: at low energies, charge transfer occurs largely in complex-mediated reactions, which give rise to both backward and forward scattering; backscattering also has a near-thermal direct contribution from long-range interactions with minimal momentum transfer. At higher collision energies, at which the complex-lifetime is much shorter than the rotational period, the direct mechanism dominates resulting

in predominantly backscattered product ions. The low- U_{RF} product velocity distribution shown for $E_T = 2.58$ eV in Figure 3, in which the drop in signal about V_{CM} indicates failure to trap products scattered at wide-angles, is also indicative of the complex-mediated mechanism as opposed to one involving a high degree of energy transfer with little kinetic energy release.

The NH_2^+/ND_2^+ reaction product is nominally the result of hydride abstraction by O^+ from NH_3/ND_3 . Formation of the $OH(OD)$ product could also involve discrete charge transfer and atom transfer steps. The similarity of form of the ND_2^+/OD^+ and charge transfer cross sections at low energies, in Figure 2, suggests that hydride abstraction competes with charge transfer. This might be expected at lower energies where the complex-mediated mechanism is observed, the complex lifetime allowing for substantial exploration of the $[D_3, N, O]^+$ phase space, including after charge transfer has occurred. The low contribution of OD^+ to the cross section at low energies, suggested above, may be expected since this channel is only slightly exothermic and may require passage through a transition state that lies above the reactants. It is interesting to note that dissociative charge transfer, giving rise to NH_2^+/ND_2^+ by dissociation of the charge transfer product, becomes possible at collision energies above 2.2 eV, and this may explain the perceptible rise in the ND_2^+/OD^+ cross section above this energy.

The issue of the relative contribution of ND_2^+ and OD^+ to the 18 amu cross section in Figure 2, unfortunately not resolved here, has broader implications. For example, if the hydride transfer channel is in fact negligible, then the TOF results in Figures 3 and 4 suggest an isotope effect that gives rise to considerably more kinetic-to-internal energy transfer in the ND_3 charge transfer reactions, as compared to the NH_3 case.

Formation of the H_3O^+ product, as per equation 6, involves the transfer of three hydrogen atoms between the heavy-atom moieties, a pathway that might be expected to occur only at low energies in a long-lived collision complex. The magnitude and energy dependence of the H_3O^+ cross section is consistent with this interpretation.

Except for the NO^+ channel, reaction of $O^+ + NH_3$ appears to yield products that are accessible on the quartet PES of the $[H_3, N, O]^+$ system, as calculated by Gonzalez, et al.⁶ If reaction is, in fact, constrained to the quartet PES, it may explain why several of the very exothermic reactions indicated in eqs 1 through 9 are not observed. Gonzalez et al. concluded that the reaction on the quartet surface was expected to be dominated by charge transfer, owing to the fact that transition states leading to other products are at energies above that of the charge transfer products.

The theoretical work also has interesting implications for the prospect of producing NO^+ in the present reaction system. Although the NO^+ product ostensibly may derive on an exothermic pathway in $O^+ + NH_3$ reactions, as indicated in eq 9, the present experiments show that this product channel gives appreciable yield only at collision energies above ~ 7 eV. On the quartet PES, all the observed complexes could be characterized as having relatively weak interactions between the heavy particle moieties, whereas the stable structures on the doublet PES were seen to have covalent N–O bonds.⁶ This suggests that the observed NO^+ product involves a crossing from quartet to doublet surface, as required by eq 9. The present experiments, however, are not conclusive on this point. Indeed, the apparent threshold for the NO^+ channel, at ~ 7 eV, is well above the collision energy required to produce this ion in its first excited state, $a(^3\Sigma^+)$.¹⁸ The formation of triplet excited NO^+ is spin-allowed. A

similar observation was made in the reactions of $N^+(^3S)$ with H_2O , in which the NO^+ channel, which at low energies proceeded on the exothermic singlet surface, was seen to undergo a sharp rise in cross section at the collision energy corresponding to access to the spin-allowed triplet PES.¹⁹

The spin conservation constraint proved important in the interpretation of the related $O^+ + CH_4$ reaction system.^{3,4} Direct dynamics calculations³ revealed that all the minor product channels observed for that system in experiments⁴ could be accounted for in spin-allowed reaction pathways. Another result of the $O^+ + CH_4$ direct dynamics work that may offer insight into the present results is that the calculations show that OH^+ derives from a stripping mechanism, involving large impact parameters and leading to forward scattered ions. If the small forward-scattered peaks in the present TOF data in Figure 3 are due to OH^+ , then it is produced in $O^+ + NH_3$ reactions by a mechanism similar to that seen in the $O^+ + CH_4$ system. These calculations also indicate that products with a C–O bond form only at small impact parameter, which may hold also for the analogous NO^+ product in the present work.

Conclusion

We have used the GIB method to study the reactions of $O^+(^4S)$ and $NH_3(\tilde{X}^1A_1)$ in the hyperthermal energy regime, obtaining absolute integral reaction cross sections as a function of collision energy from near-thermal to ~ 15 eV, as well as product velocity distributions at selected conditions. Reaction is dominated at lower energies ($E_T < 9$ eV) by charge transfer, the only channel previously detected for this system.⁵ Reactions with ND_3 allowed another major channel to be discerned, yielding ND_2^+/OD^+ throughout the energy range studied. Minor products also observed for this system included H_3O^+ at the lowest energies studied, and NO^+ , a channel that turned on only at collision energies above ~ 7 eV, and possibly H_2O^+ .

The results were discussed in light of the available theory on the $O^+ + NH_3$ system;⁶ however, interesting questions remain, notably the issue of whether crossing from the reactant quartet PES to a lower doublet surface is possible. Other questions that may be addressed, for example in direct dynamics studies, are the relative contributions of the $NH_2^+/OH^+(ND_2^+/OD^+)$ channels through the thermal and hyperthermal energy range, and isotope effects. It is hoped that the present study provides a stimulus and a useful benchmark for further theoretical investigations on the $O^+ + NH_3$ system.

Acknowledgment. This work was supported by AFOSR under Task 2303ES02. The authors wish to acknowledge Dr. A. A. Viggiano, who provided the ammonia- d_3 used in this work.

References and Notes

- (1) Ho, P. T. P.; Townes, C. H. *Annu. Rev. Astron. Astrophys.* **1983**, *21*, 239–70.
- (2) Hase, W. L.; Song, K.; Gordon, M. S. *Comput. Sci. Eng.* **2003**, *5*, 36–44.
- (3) Sun, L.; Schatz, G. C. *J. Phys. Chem. B* **2005**, *109*, 8431–8438.
- (4) Levandier, D. J.; Chiu, Y.-H.; Dressler, R. A.; Sun, L.; Schatz, G. C. *J. Phys. Chem. A* **2004**, *108*, 9794.
- (5) Smith, D.; Adams, N. G.; Miller, T. M. *J. Chem. Phys.* **1978**, *69*, 308–318.
- (6) Gonzalez, A. I.; Mo, O.; Yancz, M. *Int. J. Mass Spectrom.* **1998**, *179/180*, 77–90.
- (7) Lias, S. G.; Bartmess, J. E.; Liebman, J. F.; Holmes, J. L.; Levin, R. D.; Mallard, W. G. *J. Phys. Chem. Ref. Data* **1988**, *17*, Supplement No. 1.
- (8) Dressler, R. A.; Saller, R. H.; Murad, E. *J. Chem. Phys.* **1993**, *99*, 1159.

- (9) Qian, X.-M.; Zhang, T.; Chang, C.; Wang, P.; Ng, C. Y.; Chiu, Y.-H.; Levandier, D. J.; Miller, J. S.; Dressler, R. A.; Baer, T.; Peterka, D. S. *Rev. Sci. Instrum.* **2003**, *74*, 4096–4109.
- (10) Ikezoe, Y.; Matsuoka, S.; Takebe, M.; Viggiano, A. *Gas-Phase Ion–Molecule Reaction Rate Constants through 1986*; Mass Spectroscopy Society of Japan: Tokyo, 1987.
- (11) Levandier, D. J.; Dressler, R. A.; Chiu, Y.-H.; Murad, E. *J. Chem. Phys.* **1999**, *111*, 3954.
- (12) Ervin, K. M.; Armentrout, P. B. *J. Chem. Phys.* **1985**, *83*, 166.
- (13) Su, T.; Bowers, M. T. *Int. J. Mass Spectrom. Ion Phys.* **1973**, *12*, 347.
- (14) Su, T.; Bowers, M. T.; Classical ion–molecule collision theory. In *Gas Phase Ion Chemistry*; M. T. Bowers, Ed.; Academic Press: New York, 1979; Vol. 1.
- (15) Henglein, A. Stripping effects in ion–molecule reactions. In *Ion–Molecule Reactions in the Gas Phase*; Ausloos, P. J., Ed.; American Chemical Society: Washington, DC, 1966; Vol. 58, p 63.
- (16) Dressler, R. A.; Levandier, D. J.; Williams, S.; Murad, E. *Comments At. Mol. Phys. D* **1998**, *34*, 43.
- (17) Kimura, K.; Katsumata, S.; Achiba, Y.; Yamazaki, T.; Iwata, S. *Handbook of HeI Photoelectron Spectra of Fundamental Organic Molecules*; Halsted Press: New York, 1981.
- (18) Huber, K. P.; Herzberg, G. *Molecular Spectra and Molecular Structure IV*; Von Nostrand Reinhold Co.: New York, 1979.
- (19) Dressler, R. A.; Murad, E. *J. Chem. Phys.* **1994**, *100*, 5656.

JP803120Z